

OSCILLATING LIQUID METAL DROP UNDER UNIFORM MAGNETIC FIELD IN ZERO GRAVITY CONDITIONS

*F. Garzón*¹, *A. Figueroa*^{2*}, *S. Cuevas*¹

¹ *Instituto de Energías Renovables, Universidad Nacional Autónoma de México,
Temixco, Morelos, 62580, Mexico*

² *Conahcyt-Centro de Investigación en Ciencias, Universidad Autónoma del Estado de Morelos,
Av. Universidad 1001, Chamilpa, Cuernavaca, Morelos, 62209, Mexico*

**e-Mail: alfil@uaem.mx*

A theoretical and numerical study on the dynamics of a spherical droplet of liquid metal in zero-gravity conditions in the presence of a uniform magnetic field is presented. The droplet is initially deformed into an ellipsoidal shape and then released so that it oscillates until it recovers a spherical shape. The strength of the applied magnetic field is modulated to analyze the damping process of the oscillating droplet. An analytical solution is obtained describing the free surface evolution of the droplet considering magnetohydrodynamic effects in the creeping flow regime. A numerical simulation of the oscillating droplet is implemented by solving the three-dimensional problem using the Smoothed Particle Hydrodynamics method. The analytical and numerical results agree qualitatively and quantitatively.

Introduction.

The study of oscillating fluid drops is a classic problem in fluid mechanics. It was first studied by Sir Horace Lamb in 1932 [1], and although he had not developed an exact solution, he analyzed the oscillations of the system when the droplet interface was disturbed by some external force. It was not until 1968 when Miller and Scriven [2] had developed an exact solution that provided the viscous damping rate similar to that found by Lamb. In 2006, Wang and Joseph used the theory of viscous potential flows (VPF) to replicate the results described by Lamb with excellent results [3]. Later in 2020, a viscous fluid droplet in zero gravity oscillating around its equilibrium state due to an initial deformation was theoretically studied by Aalilija *et al.* [4]. They used the VPF theory to find the viscosity damping rate of the drop at different oscillation modes and, additionally, they also found an analytical expression of the shape of the water–gas interface. Under the same conditions, their results agree with those found by Lamb.

On the other hand, the study of drops of an electrically conducting fluid in the presence of magnetic fields has also been analyzed in the scientific literature. In 1966, disregarding viscous effects, Gailitis [5] studied the oscillating dynamics of a conducting drop in a uniform constant magnetic field. Later, in 1979, Walker and Wells [6] studied the behavior of liquid metal drops in the presence of magnetic fields. It was concluded that the resulting electromagnetic force acted in the opposite direction to the direction of the movement of the drop regardless of the sign of the imposed magnetic field gradient, acting as an electromagnetic drag [6]. In contrast to previous studies, Priede [7] assumed the viscosity to be small but non-zero and the magnetic field to be strong. This allowed the author to obtain an asymptotic solution to the eigenvalue problem for general small-amplitude three-dimensional shape oscillations. Following the approaches presented in [4, 6], in this work, magnetohydrodynamics (MHD) theory was used to study the case scenario of an oscillating liquid metal drop under a uniform magnetic field in zero

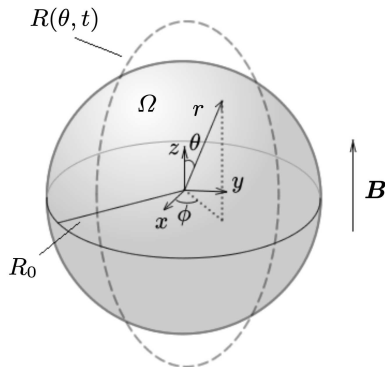


Fig. 1. Sketch of the droplet in zero gravity with the initial radius R_0 under an external magnetic field \mathbf{B} .

gravity condition. An analytical solution based on the VPF theory has been derived for the creeping-flow regime. In addition, the governing MHD equations are numerically solved using the Smoothed Particle Hydrodynamics (SPH) method. The simulation results agree quantitatively and qualitatively with the analytical solution.

1. Problem formulation. We consider a liquid metal sphere with a radius R_0 under a constant magnetic field in the vertical direction, $\mathbf{B} = B_0 \hat{z}$, under zero gravity and vacuum conditions, see Fig. 1. Initially, the droplet is deformed into an ellipsoid. Then, the droplet is released, performing a second-mode oscillation, which is attenuated by viscosity and magnetic braking. Assuming the fluid as electrically conducting, viscous, isothermal and non-magnetic, its dynamics can be modeled using the following system of equations

$$\frac{D\rho}{Dt} = -\rho (\nabla \cdot \mathbf{u}), \quad (1)$$

$$\frac{D\mathbf{u}}{Dt} = -\frac{1}{\rho} \nabla p + \nu \nabla^2 \mathbf{u} + \frac{1}{\rho} \mathbf{j} \times (\mathbf{B} + \mathbf{b}) + \gamma \kappa \delta_\epsilon \hat{n}, \quad (2)$$

$$\frac{D\mathbf{b}}{Dt} = (\mathbf{B} \cdot \nabla) \mathbf{u} + (\mathbf{b} \cdot \nabla) \mathbf{u} - (\nabla \cdot \mathbf{u}) \mathbf{B} - (\nabla \cdot \mathbf{u}) \mathbf{b} + \frac{1}{\mu_0 \sigma} \nabla^2 \mathbf{b}, \quad (3)$$

$$\mathbf{j} = \frac{1}{\mu_0} \nabla \times \mathbf{b}, \quad (4)$$

where D/Dt is the material derivative, ρ is the mass density, \mathbf{u} is the velocity vector, p is the pressure distribution, \mathbf{B} and \mathbf{b} are the external and induced magnetic fields, respectively, and \mathbf{j} is the vector of induced electric current density, while ν is the kinematic viscosity, μ_0 is the magnetic permeability of vacuum, and σ is the electrical conductivity of the fluid. Eq. (1) represents mass conservation, Eq. (2) is the Navier–Stokes equation with Lorentz and surface tension forces as source terms, Eq. (3) is the induction equation, and Eq. (4) is the Ampère’s law. In the system of Eqs. (1)–(4), it is assumed that the magnetic Reynolds number is much smaller than unity. Additionally, the induced magnetic field satisfies the following condition, $\nabla \cdot \mathbf{b} = 0$. We use the explicit curvature model, where the divergence of the unitary normal vector \hat{n} at the fluid interface may determinate the curvature κ , which is proportional to the surface tension force [8]. The

surface tension coefficient is denoted by γ and the function δ_ε reaches its maximum at the interface ($\delta_\varepsilon = 1$) and is zero in the rest of the fluid domain.

2. Analytical solution. The analytical solution is based on the theoretical approach of VPF developed by Aalilija *et al.* [4] for n -mode oscillations of a purely viscous and incompressible spherical fluid. In addition, we consider magnetohydrodynamic effects by adding the Lorentz force to the Navier–Stokes equations. The induced current density \mathbf{j} is calculated with Ohm’s constitutive law $\mathbf{j} = \sigma(\mathbf{u} \times \mathbf{B})$, assuming that the current paths are short-circuited, that is, the electric field is zero for axially symmetric flows [5]. We integrate the scalar dot product of the Navier–Stokes equation with the velocity vector over the sphere’s volume (V) to get the following energy balance equation

$$\int_V \left[\rho \frac{D\mathbf{u}}{Dt} - \nabla \cdot \bar{\boldsymbol{\tau}} \right] \cdot \mathbf{u} \, dV = \int_V [\sigma(\mathbf{u} \times \mathbf{B}) \times \mathbf{B}] \cdot \mathbf{u} \, dV, \quad (5)$$

where $\bar{\boldsymbol{\tau}}$ is the stress tensor, and the contribution of the induced magnetic field to the Lorentz force has been neglected. After some algebra and integrating the stress tensor term by parts, we get

$$\frac{D}{Dt} \int_V \frac{1}{2} \rho \mathbf{u} \cdot \mathbf{u} \, dV - \int_S \bar{\boldsymbol{\tau}} \cdot \hat{\mathbf{n}} \cdot \mathbf{u} \, dS + \int_V \bar{\boldsymbol{\tau}} : \nabla \mathbf{u} \, dV = \int_V [\sigma(\mathbf{u} \times \mathbf{B}) \times \mathbf{B}] \cdot \mathbf{u} \, dV. \quad (6)$$

Then we use the definition of stress tensor $\bar{\boldsymbol{\tau}} = 2\rho\nu\bar{\boldsymbol{\alpha}} - p\bar{\mathbf{I}}$, where $\bar{\boldsymbol{\alpha}} = \frac{1}{2}[\nabla\mathbf{u} + (\nabla\mathbf{u})^T]$ is the strain-rate tensor and $\bar{\mathbf{I}}$ is the identity tensor. For the case under study, we can assume that the strain of the gas on the liquid metal is negligible and thus consider that there is no gas surrounding the drop. We consider the dynamic boundary condition $\bar{\boldsymbol{\tau}} \cdot \hat{\mathbf{n}} = -\gamma\kappa \hat{\mathbf{n}} + p_{\text{ext}} \hat{\mathbf{n}}$, where $\kappa = -\nabla \cdot \hat{\mathbf{n}}$ is the curvature calculated at the interface S , and assume no external pressure field since the droplet is surrounded by vacuum, that is, $p_{\text{ext}} = 0$. Since no mass exchange occurs through the free surface, the kinematic interface condition is $\mathbf{u} \cdot \hat{\mathbf{n}} = v_s$, where v_s is the normal velocity of the free surface. After some algebra, the energy balance equation reads

$$\frac{D}{Dt} \int_V \frac{1}{2} \rho \mathbf{u} \cdot \mathbf{u} \, dV + \frac{D}{Dt} \int_S \gamma \, dS + \int_V 2\rho\nu\bar{\boldsymbol{\alpha}} : \bar{\boldsymbol{\alpha}} \, dV = \int_V [\sigma(\mathbf{u} \times \mathbf{B}) \times \mathbf{B}] \cdot \mathbf{u} \, dV. \quad (7)$$

The left-hand side of Eq. (7) was studied by [4], where in the pure hydrodynamic case a balance between mechanical energy and viscous dissipation was found. In the present work, we add the magnetic energy contribution to the right-hand side of Eq. (7). Aalilija *et al.* [4] described the free surface of the viscous sphere through a linear combination of Legendre polynomials, where the coefficients were time-dependent in such a way that

$$R(\theta, t) = R_0 \left(1 + \sum_n \varepsilon_n(t) P_n(\cos\theta) - \frac{\varepsilon_n^2(t)}{2n+1} \right), \quad (8)$$

where R_0 is the initial radius of the droplet, P_n denotes Legendre polynomials, and $\varepsilon_n(t)$ can be interpreted as disturbances on the free surface of the droplet. The velocity potential function is expressed as

$$\varphi(r, \theta, t) = \frac{R_0^2}{n} \left(\frac{r}{R_0} \right)^n P_n(\cos\theta) \varepsilon_n(t), \quad (9)$$

where the dot in the function $\varepsilon_n(t)$ denotes the time derivative. The velocity vector field can be obtained from the relation $\mathbf{u} = \nabla\varphi$, therefore,

$$\mathbf{u}(r, \theta, t) = R_0^{(2-n)} r^{(n-1)} \dot{\varepsilon}_n(t) \left(P_n(\cos\theta) \hat{r} - \frac{\sin\theta}{n} \frac{\partial P_n(\cos\theta)}{\partial \cos\theta} \hat{\theta} \right). \quad (10)$$

The function $\varepsilon_n(t)$ can be obtained by reducing and integrating the energy balance expressed by Eq. (7) using the free surface function R (Eq. (8)), the velocity potential φ (Eq. (9)) and the velocity field \mathbf{u} (Eq. (10)). The magnetic energy contribution can be expressed in the following way

$$\int_V [\sigma(\mathbf{u} \times \mathbf{B}) \times \mathbf{B}] \cdot \mathbf{u} \, dV \equiv \sigma \int_V (\mathbf{B} \cdot \mathbf{u})(\mathbf{B} \cdot \mathbf{u}) \, dV - \sigma \int_V (\mathbf{B} \cdot \mathbf{B})(\mathbf{u} \cdot \mathbf{u}) \, dV, \quad (11)$$

where

$$\begin{aligned} \sigma \int_V (\mathbf{B} \cdot \mathbf{u})(\mathbf{B} \cdot \mathbf{u}) \, dV &= \sigma B_0^2 R_0^4 \int_V \left(\frac{r^{n-1}}{R_0} \right)^2 \dot{\varepsilon}_n^2 P_{n-1}^2(\cos\theta) \, dV \\ &\approx \sigma B_0^2 4\pi R_0^5 \left(\frac{1}{2n+1} \right) \left(\frac{1}{2n-1} \right) \dot{\varepsilon}_n^2, \end{aligned} \quad (12)$$

and

$$\begin{aligned} \sigma \int_V (\mathbf{B} \cdot \mathbf{B})(\mathbf{u} \cdot \mathbf{u}) \, dV &= \sigma B_0^2 2\pi \int_0^\pi \varphi \frac{\partial \varphi}{\partial r} R^2 \sin\theta \, d\theta, \\ &\approx \sigma B_0^2 4\pi R_0^5 \left(\frac{1}{n(2n+1)} \right) \dot{\varepsilon}_n^2, \end{aligned} \quad (13)$$

therefore,

$$\int_V \sigma((\mathbf{u} \times \mathbf{B}) \times \mathbf{B}) \cdot \mathbf{u} \, dV \approx \sigma B_0^2 4\pi R_0^5 \left(\frac{1}{2n+1} \right) \left(\frac{1}{2n-1} - \frac{1}{n} \right) \dot{\varepsilon}_n^2. \quad (14)$$

The terms of the hydrodynamic contribution in Eq. (7) can be consulted in [4]. Then, the function $\varepsilon_n(t)$ satisfies the following equation

$$\ddot{\varepsilon}_n + 2(\Lambda_n + \lambda_n)\dot{\varepsilon}_n + \omega_n^2 \varepsilon_n = 0, \quad (15)$$

where the coefficients ω_n , λ_n and Λ_n are defined as

$$\omega_n = \sqrt{n(n-1)(n+2)} \frac{\gamma}{\rho R_0^3}, \quad \lambda_n = (2n+1)(n-1) \frac{\nu}{R_0^2}, \quad \Lambda_n = \left(\frac{n-1}{4n-2} \right) \frac{\sigma B_0^2}{\rho}, \quad (16)$$

with B_0 being the magnitude of the applied magnetic field, ω_n is the angular frequency of the oscillation, λ_n is the viscous dissipation rate, and Λ_n is the magnetic dissipation rate. Note that Λ_n coincides with the magnetic dissipation rate found by Gailitis [5] and λ_n with the viscous dissipation rate found by Priede [7]. The solution of Eq. (15) depends

on the discriminant value $\Delta_n = (\lambda_n + \Lambda_n)^2 - \omega_n^2$. For the damped regime $\Delta_n < 1$, the function $\varepsilon_n(t)$ is

$$\varepsilon_n(t) = \left(\left(\frac{\dot{\varepsilon}_n^0 + (\lambda_n + \Lambda_n)\varepsilon_n^0}{\sqrt{-\Delta_n}} \right)^2 + (\varepsilon_n^0)^2 \right)^{1/2} e^{-(\lambda_n + \Lambda_n)t} \cos(\sqrt{-\Delta_n}t + \psi), \quad (17)$$

where

$$\tan \psi = -\frac{\dot{\varepsilon}_n^0 + (\lambda_n + \Lambda_n)\varepsilon_n^0}{\varepsilon_n^0 \sqrt{-\Delta_n}}.$$

For the over-damped regime $\Delta_n > 1$, the solution of Eq. (15) reads

$$\varepsilon_n(t) = \left(\varepsilon_n^0 \cosh(\sqrt{\Delta_n}t) + \frac{\dot{\varepsilon}_n^0 + (\lambda_n + \Lambda_n)\varepsilon_n^0}{\sqrt{\Delta_n}} \sinh(\sqrt{\Delta_n}t) \right) e^{-(\lambda_n + \Lambda_n)t}. \quad (18)$$

Finally, for the critical regime $\Delta_n = 0$, the solution for $\varepsilon_n(t)$ is

$$\varepsilon_n(t) = [\varepsilon_n^0 + (\dot{\varepsilon}_n^0 + (\lambda_n + \Lambda_n)\varepsilon_n^0)t] e^{-(\lambda_n + \Lambda_n)t}, \quad (19)$$

here ε_n^0 and $\dot{\varepsilon}_n^0$ are constants obtained from the initial conditions.

3. Numerical solution. The set of Eqs. (1)–(4) is named as “The Fundamental Equations of Smoothed Particle Magnetohydrodynamics (SPMHD) for a weakly compressible fluid” [9]. They were solved numerically by the SPH method. The code is home-made in Fortran 90 and parallelized with CUDA, where each thread represents a unique particle ID. The Euler method was used for the temporal term, and the time step was chosen to satisfy the CFL condition for an electrically conducting fluid [9]. A spherical fluid volume of radius $R_0 = 1$ mm was simulated through a uniform distribution of SPH particles. A Spike 3D kernel with a smoothing length of $h = 2\Delta l$, where Δl is the initial particle spacing [10] and an artificial sound speed of $c_0 = 15$ m/s were chosen. The spherical shape of the droplet was created through a sugarcubed representation with 7.1×10^4 particles. Finally, in the SPH framework, all variables satisfy the Neumann boundary condition at the free surface, except the induced magnetic field which is forced to be zero.

4. Results. The dynamics of the oscillating liquid metal droplet in zero gravity conditions and without an external magnetic field can be seen in Fig. 2. From Eq. (10), the initial velocity profile \mathbf{u}_i is established for a two-mode droplet $n = 2$, that is, $\mathbf{u}_i(x, y, z, t) = \dot{\varepsilon}_2(t)(-0.5x, -0.5y, z)$. In the damped regime $\dot{\varepsilon}_2(t=0) = -\dot{\varepsilon}_2^0$, with $\varepsilon_n^0 = 0$ and $\dot{\varepsilon}_2^0 = 100 \text{ s}^{-1}$. Initially, the drop is spherical (Fig. 2a), then the droplet is deformed into an ellipsoidal shape, where the equatorial region is expanded and the polar regions

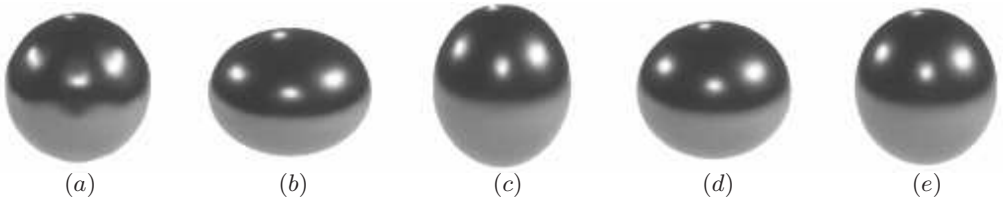


Fig. 2. Snapshots of the oscillating drop without magnetic field. (a) $t = 0$. (b) $t = 3$ ms. (c) $t = 7.2$ ms. (d) $t = 14.4$ ms. (e) $t = 19.2$ ms. $Re = 5$ and $Ha = 0$. Numerical simulations.

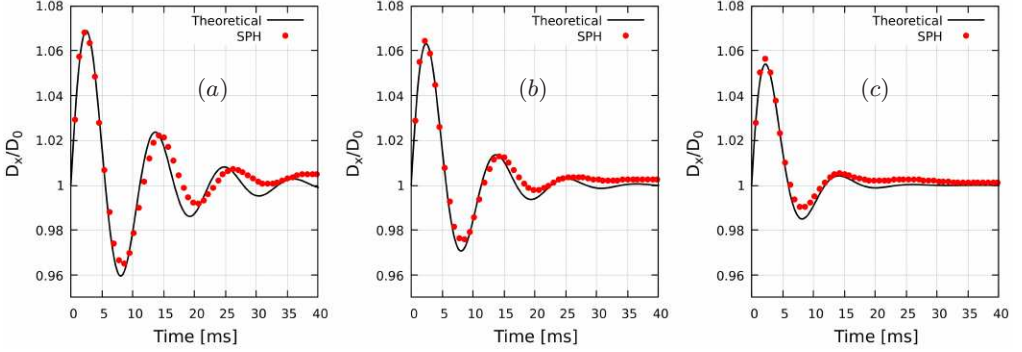


Fig. 3. Evolution of the diameter at the equator's droplet for $Re=5$. (a) $Ha=0$. (b) $Ha=4$. (c) $Ha=9$. Continuous lines: analytical solution from Eq. (8). Markers: numerical simulations.

are contracted (Fig. 2b) and then released so that it oscillates with the mode $n=2$ (Figs. 2c,d), until it recovers the spherical shape. The dynamics is characterized through the Reynolds and Hartmann numbers, defined as $Re = u_m R_0 / \nu$ and $Ha = B_0 R_0 \sqrt{\sigma / \rho \nu}$, respectively, where u_m is the maximum magnitude of the velocity when the droplet is initially deformed. In Fig. 2, $Re = 5$ and $Ha = 0$, thus, convection slightly dominates over diffusion and no magnetic effects are present.

In order to quantify the observations in Fig. 2, the dimensionless diameter of the droplet, $D = D_x / D_0$, where $D_0 = 2R_0$ and D_x is the length in the x -direction at the equator of the droplet, is plotted as a function of time in Fig. 3a. Initially, the value of the dimensionless diameter is unity, then it expands and stretches due to mass conservation, converting kinetic energy into potential energy and vice-versa, while the energy of the droplet decreases due to viscous dissipation until it reaches the state of low energy, that is, the spherical shape. As the Hartmann number increases, the magnetic braking also increases, and the droplet oscillation is strongly attenuated, as observed in Figs. 3b,c. The latter can be appreciated with a snapshot of the droplet in Fig. 4. Even if the analytical solution is valid for the creeping flow regime ($Re < 1$), it agrees qualitatively and quantitatively with the three-dimensional numerical calculations in the laminar regime, as seen in Fig. 3. In order to compare with the numerical solutions, we opted for using $Re=5$, since the numerical methodology does not allow Re to be smaller.

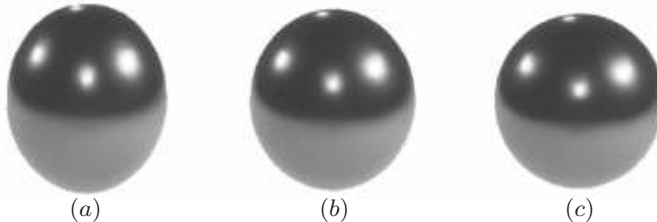


Fig. 4. Snapshots of the oscillating droplet for $Re=5$ at $t=14.4$ ms. (a) $Ha=0$. (b) $Ha=4$. (c) $Ha=9$. Numerical simulations.

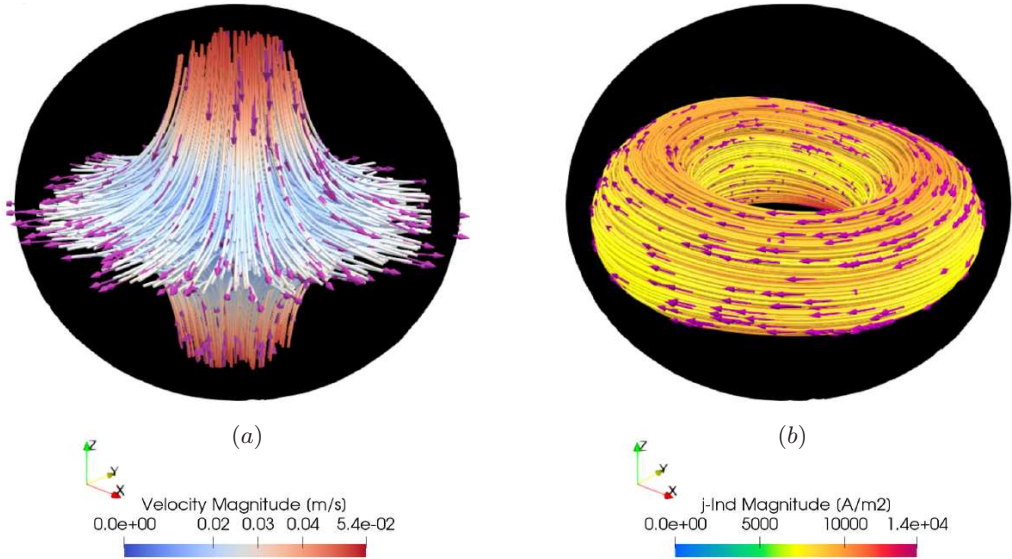


Fig. 5. Isometric view of (a) instant streamlines and (b) instant path of the induced electric current inside the drop for $Re=5$ and $Ha=9$ at $t=1$ ms. The black backdrop denotes the footprint of the droplet. Numerical simulations.

The three-dimensional structure of the flow field inside the droplet along with the induced electric current can be observed in Figs. 5a,b, respectively. Shortly after the initial state ($t=1$ ms), the droplet is deformed into an ellipsoidal shape by internal flows departing from the poles and colliding in the equatorial region, see Fig. 5a, which coincides with the initial velocity condition \mathbf{u}_i . These flows interact with the applied magnetic field and generate loops of induced electric current inside the droplet, see Fig. 5b. As observed in Fig. 5, the droplet expands in the equatorial region and, as the oscillation continues, the polar region will extend, as seen in Fig. 4. At this instant, the flow and the induced electric current will inverse their directions. Under the working conditions, the Joule effect (\mathbf{j}^2/σ) can be ignored.

5. Concluding remarks. The oscillations that occur on a liquid metal sphere deformed by an initial irrotational velocity field in the absence of gravity under a uniform constant magnetic field were studied theoretically and numerically in the linear regime. The theoretical analysis determines the magnetic damping rate from the energy balance equation when the Lorentz force is incorporated. In addition to viscous dissipation, energy is also dissipated by magnetic braking due to the induced electric currents circulating in the drop. The oscillations of the interface decrease in amplitude as the intensity of the magnetic field increases, which is characterized by the Hartmann number. Three-dimensional numerical simulations based on SPMHD agree qualitatively and quantitatively with the analytical solution. Considering its lower vapor pressure and toxicity, Galinstan meets all the requirements as a working fluid in the present study.

Acknowledgments.

This work was supported by DGAPA-UNAM under project IN107921 and by Fundaci3n Marcos Moshinsky. F.Garz3n thanks a PhD grant from Conahcyt. Finally,

A. Figueroa thanks the program Investigadoras e Investigadores por México from Conahcyt.

References

- [1] H. LAMB. *Hydrodynamics*. (Cambridge University Press, 1945).
- [2] C. A. MILLER AND L.E. SCRIVEN. The oscillations of a fluid droplet immersed in another fluid. *Journal of Fluid Mechanics*, vol. 32 (1968), no. 3, p. 417–435.
- [3] J. WANG AND D.D. JOSEPH. Purely irrotational theories of the effect of the viscosity on the decay of free gravity waves. *Journal of Fluid Mechanics*, vol. 559 (2006), p. 461–472.
- [4] A. AALILJA, C.-A. GANDIN, AND E. HACHEM. On the analytical and numerical simulation of an oscillating drop in zero-gravity. *Computers and Fluids*, vol. 197 (2020), p. 104362.
- [5] A. GAILITIS. Oscillations of a conducting drop in a magnetic field. *Magnetohydrodynamics*, vol. 2 (1966), no. 2, pp. 79–90.
- [6] J.S. WALKER AND W.M. WELLS. Drag force on a conductive spherical drop in a nonuniform magnetic field. *Technical Rep. ORNL/TM-6976*, (1979).
- [7] J. PRIEDE. Oscillations of weakly viscous conducting liquid drops in a strong magnetic field. *Journal of Fluid Mechanics*, vol. 671 (2011), pp. 399–416.
- [8] J. BRACKBILL, D. KOTHE, AND C. ZEMACH. A continuum method for modeling surface tension. *Journal of Computational Physics*, vol. 100 (1992), no. 2, pp. 335–354.
- [9] J. AL-SALAMI, C. HU, M.M. KAMRA, AND K. HANADA. Magnetic induction and electric potential smoothed particle magnetohydrodynamics for incompressible flows. *International Journal for Numerical Methods in Fluids*, vol. 93 (2021), no. 3, pp. 720–747.
- [10] F.V. SIROTKIN AND J.J. YOH. A new particle method for simulating breakup of liquid jets. *Journal of Computational Physics*, vol. 231 (2012), no. 4, pp. 1650–1674.

Received 24.11.2024